

THEORETICAL STUDY OF THERMALLY DRIVEN HEAT PUMPS BASED ON DOUBLE ORGANIC RANKINE CYCLE: WORKING FLUID COMPARISON AND OFF-DESIGN SIMULATION

*Jonathan Demierre, Daniel Favrat, Industrial Energy Systems Laboratory (LENI)
Ecole Polytechnique Fédérale de Lausanne (EPFL), 1015 Lausanne, Switzerland
jonathan.demierre@a3.epfl.ch*

*This paper was published in the proceedings of the 10th International Heat Pump Conference 2011
(www.heatpumpcentre.org/en/hppactivities/ieaheatpumpconference).*

Abstract: This study deals with a type of thermally driven heat pumps that consists of a reverse Rankine heat pump cycle, the compressor of which is driven by the turbine of a supercritical Organic Rankine Cycle (ORC). The application is residential heating (domestic hot water and floor heating) of small buildings requiring a cumulated thermal power of approximately 40 kW. An approach that enables the comparison of performance that can be expected with different working fluids is presented. It appears that R134a, R1234yf, R227ea and R236fa are among the best candidates. An off-design simulation tool of such thermally driven heat pumps has been implemented that includes both turbine and compressor off-design models. This thermally driven heat pump model has been used to predict the performance of an existing experimental prototype about to be tested.

Key Words: thermally driven heat pumps, ORC, off-design, radial turbine, oil-free

1 INTRODUCTION

Nowadays environmental and global warming concerns, increasing costs, potential shortage of fossil fuels and the need for a more efficiency conversion of biofuels stimulate the development of equipment for a more rational use of energy. One of the solutions is the improvement of the energy conversion for heating and cooling in particular. Concerning heating, the main alternatives are linked to using heat pumps, which enable a use of renewable energy from the environment.

The present heat pump market is dominated by two main categories of heat pumping systems: the electrically driven compression heat pumps, which are the most widely used, and the thermally driven heat pumps. The thermally driven heat pumps are usually realized with absorption cycles. These cycles are based on two pressure and three temperature levels, the driving exergy power being the heat exergy provided at the highest temperature level to the generator (Borel and Favrat 2010). Note that to the category of thermally driven heat pumps we can also add systems made of a compression heat pump, the compressor of which is directly or indirectly driven by a heat engine, usually an internal combustion engine.

The system studied in this work is a thermally driven hermetic heat pump that consists of a compression heat pump and an organic Rankine cycle (ORC) in which the turbine is directly driving the compressor. The condenser is common to both cycles (see Figure 1). The vapor generation of the Rankine cycle is pictured as a supercritical process, but it could equally be subcritical. However the preliminary results (Demierre and Favrat 2008) show that it is particularly interesting to have a supercritical evaporation. As the compression heat pump cycle is a reversed organic Rankine cycle, this system is called here an ORC-ORC heat

pump. Like absorption heat pumps, ORC-ORC systems have the advantage of being able to operate with a variety of fuels or heat sources like wood pellets, natural gas, solar heat, geothermal heat or waste heat. An earlier concept of gas driven ORC-ORC heat pump using the same working fluid in both cycles and a dynamic compressor and turbine rotating on refrigerant vapour bearings was proposed by Strong (Strong 1980), but difficulties were encountered which could have been caused by the lack of appropriate materials. Moreover, an additional point that penalized such a system was the problematic of the CFC refrigerants, which were, at the time, among the best candidates for high temperature cycles. Progress in materials, bearing knowledge and new ozone depletion free refrigerants having a reasonably high temperature chemical stability and/or acceptance, allow the reconsideration of this approach. The recent demonstration of one concept of miniature high speed (about 210 krpm) centrifugal compressor directly driven by an electric motor rotating on refrigerant gas bearings (Schiffmann and Favrat 2009) opens the way to such devices with or without electric motor.

The concept studied in this work is a low power system (for small buildings) with a single-stage radial compressor and a single-stage radial inflow turbine. The compressor and turbine are directly coupled on the same shaft rotating on refrigerant vapor gas bearings. This gives the system the advantage of being oil-free, fully hermetic and with low maintenance costs. Because of the characteristics of dynamic compressors and turbines a low density fluid is preferred and refrigerant HFC-134a has been selected at this stage. It is chemically stable at relatively high temperatures (at least up to 200°C), particularly in an oil-free environment.

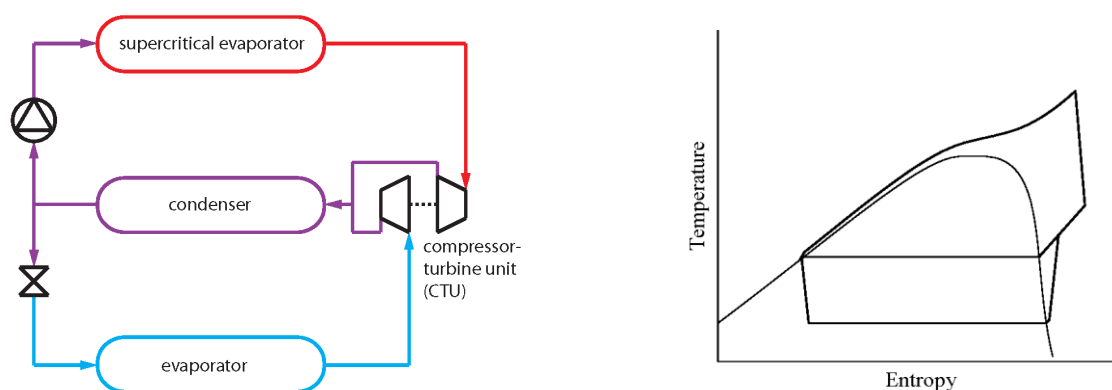


Figure 1: Schematic flowsheet and T-s diagram of a simple ORC-ORC heat pump unit

2 WORKING FLUID COMPARISON

2.1 Approach

In previous developments, a tool has been developed to evaluate the potential of ORC-ORC systems for residential heating applications (Demierre and Favrat 2008). The approach used to evaluate the performances of ORC-ORC systems is summarized in Figure 2.

The first step of the computation process is the calculation of the cycles (the thermodynamic properties at all points and the mass flows in the Rankine cycle and the heat pump). The thermodynamic properties of the refrigerant are calculated with *REFPROP* (Lemmon et al. 2010).

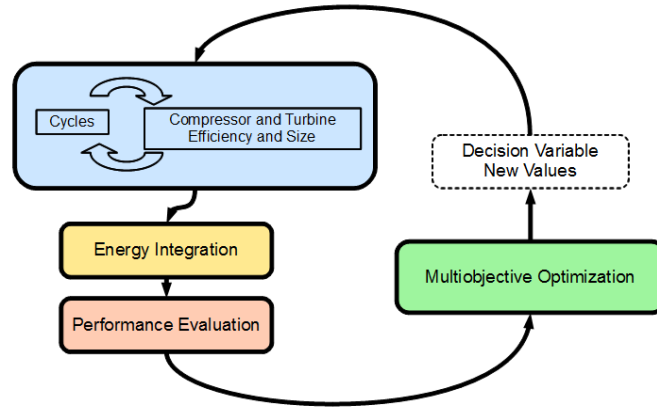


Figure 2: Diagram of the ORC-ORC design and optimization tool

A polynomial approximation of the correlation of (Rohlik 1968) is used to model the turbine isentropic efficiency η_T . This relation gives the maximum efficiency that can be achieved for a fixed turbine specific speed n_{sT} :

$$n_{sT} = \frac{\omega \dot{V}_T^{1/2}}{\Delta h_{0sT}^{3/4}} \quad (1)$$

with \dot{V}_T : the volumetric flow at the turbine outlet
 ω : the angular velocity
 Δh_{0sT} : the isentropic enthalpy difference between the inlet and outlet of the turbine

The compressor isentropic efficiency η_C is modelled using a similar method. A correlation adapted from (Balje 1981) by (Whitfield and Baines 1990) that relates the maximum efficiency to the compressor specific speed n_{sC} is approximated. The compressor specific speed is defined by

$$n_{sC} = \frac{\omega \dot{V}_C^{1/2}}{\Delta h_{0sC}^{3/4}} \quad (2)$$

with \dot{V}_C : the volumetric flow at the compressor inlet
 ω : the angular velocity
 Δh_{0sC} : the isentropic enthalpy difference between the outlet and inlet of the compressor

The optimal turbine and compressor wheel diameters, respectively D_{2T} and D_{2C} , can be roughly estimated using the relations:

$$n_{sT} d_{sT} = 2 \quad \text{where } d_{sT} = \frac{D_{2T} \Delta h_{0sT}^{1/4}}{\dot{V}_T^{1/2}} \quad \text{for the turbine} \quad (3)$$

$$n_{sC} d_{sC} = 3 \quad \text{where } d_{sC} = \frac{D_{2C} \Delta h_{0sC}^{1/4}}{\dot{V}_C^{1/2}} \quad \text{for the compressor} \quad (4)$$

Those relations approximate the lines of best efficiency of the $n_s - d_s$ diagrams from (Balje 1981).

Once the cycles have been determined, the mass flows of the heat sources and the heat sinks (hot domestic water and heating water) have to be optimally set, which is the energy integration step. The energy integration of the system is made using an in-house software tool based on the pinch analysis method. The mass flows of the heat sources and the heat sinks are calculated by solving a problem of operating cost minimization. The stream costs are set in order that the operating cost is minimal when the COP is maximal. The heat service cost is set negative, the hot source (the fumes) cost is set positive and the cost of the cold source (the glycol water) is equal to 0 as it is considered as a free resource. The ratio between the heat service cost and the hot source cost is set in order that the hot source power is increased only if the heat service power increases faster. In other words, this avoids using the fumes to only heat directly the water.

The performance of the system is characterized by the overall coefficient of performance (COP) that is defined as the ratio of the heat rate supplied and the power consumed by the system that is not free of charge:

$$COP = \frac{\dot{Q}_W^-}{\dot{Q}_{fumes}^+ + \frac{\dot{E}_p^+}{0.56}} \quad (5)$$

where \dot{Q}_W^- is the heat rate supplied (hot water and heating), \dot{Q}_{fumes}^+ is the heat provided by the fumes resulting from the combustion of natural gas (assumed to be 100% methane) and \dot{E}_p^+ is the electrical power consumed by the ORC-ORC pump (which is the only electrical power consumed by the ORC-ORC). \dot{E}_p^+ is divided by 0.56 to take into account for the efficiency of a modern combined cycle power plant that produces this electrical power from the same fuel, in order to define a COP which is strictly based on the conversion of the fuel (here, methane) into heat.

An in-house multiobjective optimization tool, MOO (Molyneaux et al. 2010), based on an evolutionary algorithm is used to find optimal sets of design parameters, that are the temperature and pressure levels of the cycles and the rotational speed of the compressor-turbine unit (CTU). This optimization is done with the COP maximization as the first objective and the rotational speed of the CTU as the second objective. The CTU rotational speed is chosen as the second objective, because for low power compressor and turbine the optimal rotational speed becomes critically high. The coupling of the different software programs is performed thanks to an in-house energy system optimization platform, OSMOSE (Marechal et al. 2004).

2.2 Results

A study was made on a system using R134a as working fluid (Demierre and Favrat 2008). The hot heat source consists of the fumes coming from a stoichiometric combustion of methane that can be cooled down to 4°C and the cold heat source is the brine of a ground source that cools down from 4°C to 1°C. The heating services are the production of domestic hot water (from 10°C to 60°C) and heating water for floor heating (from 30°C to 35°C). The

total power of the heating services is about 40 kW with a distribution of 80% for the heating system of the building and 20% for domestic hot water, which is typical for the winter season.

A similar study has been made for different working fluids that are commonly used or expected to be good candidates for heat pump, refrigeration or ORC applications. Two-objective optimizations with the COP and the CTU rotational speed as objectives are made and the resulting Pareto curves are shown in Figure 3. The Pareto curve (or Pareto front) of a two-objective optimization can be plotted in a 2-D graph with the two objectives on the respective axis. The Pareto front divides the solution domain into two sub-domains: the sub-domain of unfeasible solutions and the sub-domain of sub-optimal solutions. For a solution located on the Pareto curve, it is not possible to find another solution that improves both objectives. Each point of the Pareto front is an optimal solution. The optimization algorithm does not eliminate systematically all the points that are not near the Pareto front. Nevertheless, those points are clearly not optimal solutions and as such can be ignored. It can be seen that R410A (orange points) is not a good candidate because the maximum COP is about 2.16 and the CTU rotational speed N for this value of COP is excessive. A large number of refrigerants show more or less the same results with a maximum COP between 2.2 and 2.4 for a rotational speed between 200 krpm and 250 krpm. However, in this group of fluids, R134a (green points), R1234yf (red points) and Isobutan (dark blue points) are the best candidates, as their curve is shifted to the right compared to the others. At this stage, the best candidates seem to be R227ea (dark purple points) with a COP of 2.36 at about 163 krpm, R236fa (dark green points) with a COP of 2.40 at about 160 krpm and R245fa (brown points) with a COP of 2.45 at about 142 krpm.

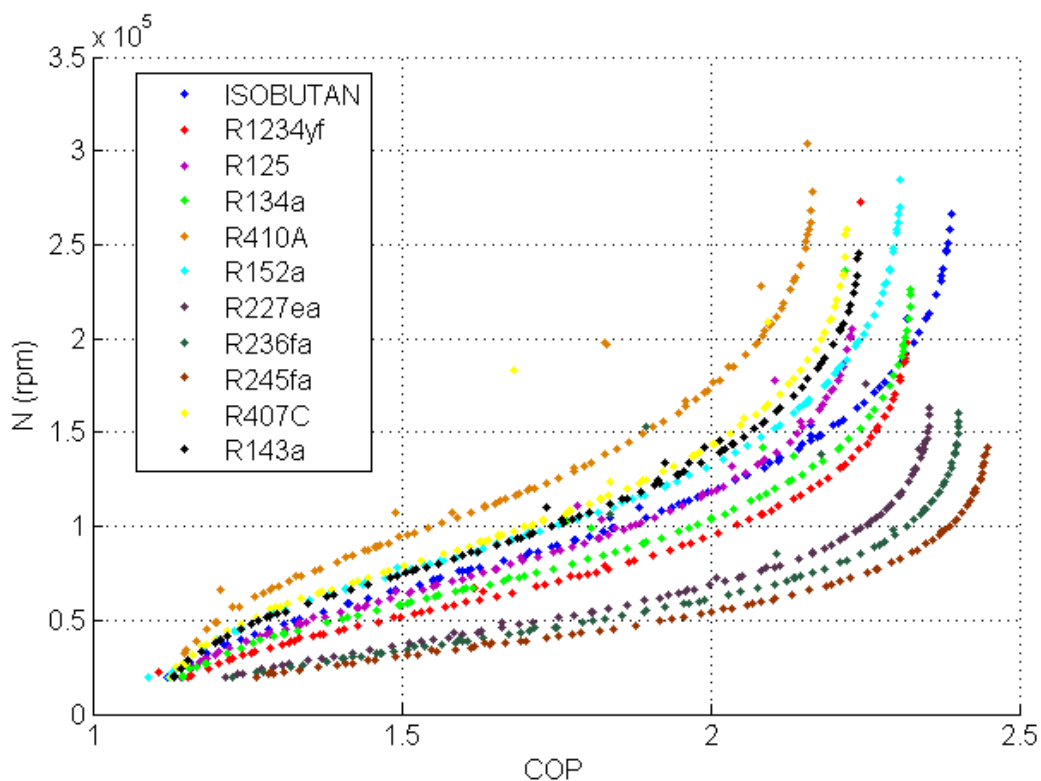


Figure 3: Pareto curves resulting from optimizations with maximization of the COP as first objective and minimization of the CTU rotational speed as second objective for different working fluids

R134a, R1234yf, R227ea, R236fa and R245fa are compared in Table 1 by looking at several key parameters. Even if Isobutan enables to reach a high COP, it is eliminated because of its flammability. It has to be noted that the evaporation pressure (which corresponds to a temperature of about 0°C) of the heat pump cycle for R245fa is below the atmospheric

pressure. This is an important disadvantage, since the working fluid could be contaminated with ambient air, if the system happens not to be totally hermetic. The compressor and turbine wheel diameters are in the range 20 mm to 45 mm, which is not problematic regarding the machining with today's technology. A reason that can explain why R227ea, R236fa and R245fa are better is the shaft losses that are lower with a lower rotational speed. It can be seen in Table 1 that the shaft losses are 53% lower with R227ea, 63% lower with R236fa and 77% lower with R245fa than with R134a. With R236fa and R245fa, a turbine pressure ratio of respectively 13.1 and 18.6 are obtained, which cannot realistically be achieved with a one stage radial machine. It has to be mentioned that this approach of modeling the compressor and turbine efficiencies as functions of the specific speed does not take into account the effect of the pressure ratio. In reality, the compressor and turbine efficiency are negatively affected by too high pressure ratios and thus, the COP for R236fa and R245fa should be lower than the predicted value with this approach.

Table 1: Comparison of the design parameter values for different working fluids

		R134a	R1234yf	R227ea	R236fa	R245fa
N	(krpm)	226	198	163	160	142
COP	(-)	2.33	2.32	2.36	2.40	2.45
Compressor wheel diameter	(mm)	21	21	23	26	33
Turbine wheel diameter	(mm)	21	22	23	27	34
HP evaporation pressure	(bar)	2.9	3.2	2.0	1.1	0.53
Condensing pressure	(bar)	9.1	9.1	6.3	3.9	2.2
ORC evaporation pressure	(bar)	77	70	62	51	41
Compressor pressure ratio	(-)	3.1	2.8	3.2	3.5	4.2
Turbine pressure ratio	(-)	8.5	7.7	9.8	13.1	18.6
Shaft losses	(W)	115	91	54	42	27

At this stage, the best candidates seem to be R134a, R1234yf, R227ea and R236fa. R245fa is eliminated for this application because its pressure at the heat pump evaporation is below the atmospheric pressure. It has to be mentioned that some of the tested working fluids exhibit a slope of the saturation curve that is positive at the saturated vapor side in a T-s diagram, which implies that a sufficient superheating before the compressor is required in order to avoid crossing the saturation line during compression. This is of course taken into account in this analysis.

3 OFF-DESIGN MODELING

The aim of the off-design modeling is to predict the system performance for a given compressor-turbine unit geometry. In this work, the other parts of the system (heat exchangers, pump, expansion valve and pipes) are not modeled in detail, which means that the inputs and outputs of each component are simply set by the user or calculated using the equations of conservation of mass and energy. The CTU model must allow the prediction of the efficiency and the capacities of the compressor and turbine that are required to calculate the thermodynamic cycles. The modeling approach that is used for the compressor and the turbine is the mean line or one-dimensional modeling. This consists of predicting the performance of the turbomachine by calculating the flow properties along the mean stream line of the channels. The implementation of the compressor and shaft loss models was a part of a previous PhD thesis (Schiffmann 2008) and so, modeling details on those elements are not presented in this paper. The radial turbine model is described in the following subsection.

3.1 Radial Turbine Model

The approach that is used to model the turbine is the one described by Baines in (Moustapha et al. 2003). The flow properties are calculated at the inlet and exit of each element of the

turbine along the mid-streamline. Figure 4 shows the layout of a radial inflow turbine and the locations that are considered to calculate the flow. Each element of the turbine is calculated one after the other in the direction of the flow. The model does not include the modeling of the volute. It is assumed that the flow velocity is low in this element and thus, the losses can be neglected.

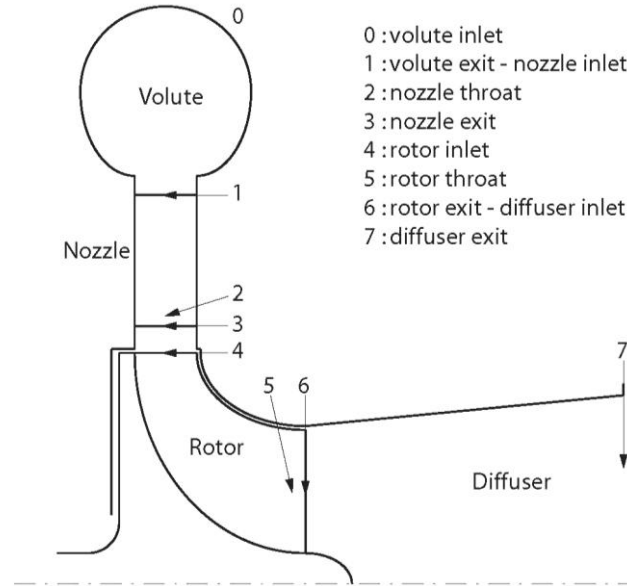


Figure 4: Radial turbine layout and locations that are considered for the mean line model

Nozzle

The nozzle throat is usually the first location at which the flow chokes and therefore, the nozzle throat area is an important parameter to set the turbine flow capacity. In order to calculate the flow properties at this location, the loss that occurs between nozzle inlet and throat is expressed using a static enthalpy loss coefficient:

$$\xi = \frac{h_2 - h_{2s}}{\frac{1}{2}C_2^2} \quad (6)$$

where C_2 is the absolute flow velocity at the nozzle throat. To estimate this loss coefficient, a modified expression of the correlation of Rodgers proposed by Baines (Baines 2006) is used:

$$\xi = \frac{0.05}{Re^{0.2}} \left(\frac{\tan^2 \alpha_{b3}}{s_{noz} / c_{noz}} + \frac{o_{noz}}{b_3} \right) \quad (7)$$

where α_{b3} is the blade exit angle, s_{noz} is the blade spacing at exit, c_{noz} is the blade chord length, o_{noz} is the throat opening and b_3 is the blade exit high. The same procedure is used to calculate the loss from the nozzle inlet to the rotor inlet. The flow deviation at the nozzle exit is modelled by calculating the exit flow angle α_3 with the cosine rule expressed with the passage areas and the aerodynamic blockage coefficients:

$$\alpha_3 = \arccos \left(\frac{A_{th,noz} (1 - B_{th,noz})}{A_3 (1 - B_3)} \right) \quad (8)$$

where $A_{th,noz}$ is the nozzle throat area, A_3 is the annulus exit area, and $B_{th,noz}$ and B_3 are the blockage coefficients respectively at throat and exit. If the nozzle is not choked, the flow angle at rotor inlet is assumed to be equal to the flow angle at nozzle exit. If the nozzle is choked, supersonic expansion can occur in the nozzle-rotor interspace which turns the flow in the meridional direction.

Rotor

The internal losses in the rotor are modelled by a sum of four contributions: the incidence loss, the passage loss, the tip clearance loss and the trailing edge loss.

The incidence loss is related to the work that is needed to turn the flow in the required direction when entering into the rotor. The expression proposed by (Wasserbauer and Glassman 1975) is implemented in the model:

$$\Delta h_{inc} = \frac{1}{2} W_4^2 \sin^2 \beta_4 - \beta_{4,opt} \quad (9)$$

where W_4 is the relative flow velocity at rotor inlet, β_4 is the relative flow angle at rotor inlet and $\beta_{4,opt}$ is the optimal incidence angle which is usually between -20° and -40° (Moustapha et al. 2003).

The passage losses include the loss due to secondary flows and the loss due to friction on the walls. The correlation that is implemented in the model is a simple model based on the mean kinetic energy of the working fluid. The expression that is used was proposed by (Wasserbauer and Glassman 1975):

$$\Delta h_{pass} = \frac{1}{2} K_{pass} W_4^2 \cos^2 \beta_4 - \beta_{4,opt} + W_6^2 \quad \text{with} \quad K_{pass} = 0.3 \quad (10)$$

where K_{pass} is a coefficient that has to be determined with experimental data and W_6 is the relative flow velocity at turbine outlet.

The tip clearance loss is due to the leakage of the flow in the gap between rotor tip and shroud. The expression that is implemented is the one given by Baines in (Moustapha et al. 2003):

$$\Delta h_{cl} = \frac{U_4^3 N_b}{8\pi} K_x \varepsilon_x C_x + K_r \varepsilon_r C_r + K_{xr} \sqrt{\varepsilon_x \varepsilon_r C_x C_r} \quad (11)$$

with $C_x = \frac{1 - r_{6t}/r_4}{C_{m4} b_4}$ and $C_r = \left(\frac{r_{6t}}{r_4} \right) \frac{l_{rot} - b_4}{C_{m6} r_{6rms} b_6}$

where U_4 is the rotor tip velocity, N_b is the blade number, ε_x and ε_r are respectively the axial and radial clearances, r_{6t} is the tip radius at the exit, r_4 is the radius at the inlet, b_4 is the inlet blade height, C_{m4} and C_{m6} are the meridional component of the absolute velocity respectively at inlet and exit, l_{rot} is the axial length of the rotor, b_6 is the exit blade height and r_{6rms} is the mean radius at exit. K_x , K_r and K_{xr} are empirical coefficients and values of respectively 0.4, 0.75 and -0.3 are recommended from test data.

This trailing edge loss is due to the flow separation at the blade trailing edge that creates a region of lower pressure just behind the blade. To evaluate this loss, a simple correlation recommended by Baines (Baines 2006) that is based on axial turbine test data is used:

$$\Delta h_{TE} = \frac{1}{2} C_6^2 K_{TE} \frac{t_{TE}}{o_{rot}} \quad \text{with} \quad K_{TE} = 0.2 \quad (12)$$

where K_{TE} is an empirical coefficient, C_6 is the absolute flow velocity at the exit, t_{TE} is the blade trailing edge thickness and o_{rot} is the throat opening.

The exit flow angle deviation is calculated in the same way as for the nozzle (Eq. 8) using the cosine rule. If the rotor throat is choked, a supersonic expansion can occur at the trailing edge that turns the flow in the axial direction. An additional external loss related to the rotor, the windage loss, is taken into account in the modeling. This loss is due to the friction in the gap between the rotor back face and the back plate. This loss acts as a loss of power on the turbine shaft.

Diffuser

The aim of the diffuser is to enable the recovery of a part of the kinetic energy of the flow that leaves the rotor. In this model, it is assumed that the angular momentum is constant, which is expressed by:

$$rC_\theta = \text{cte} \quad (13)$$

where C_θ is the tangential component of the flow absolute velocity. The implemented loss model is due to Japikse (Moustapha et al. 2003) who gives a correlation for the diffuser efficiency defined as the ratio of the real and ideal pressure recovery coefficients, respectively C_p and C_{pi} :

$$\eta_{dif} = \frac{C_p}{C_{pi}} = \frac{P_7 - P_6 / P_{06} - P_6}{P_{7s} - P_6 / P_{06} - P_6} \quad (14)$$

The correlation proposed by Japikse is based on the examination of a large database and is expressed by the product of the different contributions:

$$\eta_{dif} = \eta_{AR} \eta_\alpha \eta_B$$

(15)

with

$$\eta_{AR} = 0.72 + 3.0 \exp^{-0.9 - 1.5 A_7 / A_6} \quad \text{area ratio effect}$$

$$\eta_\alpha = 1.1 - 0.0001 \alpha_6^{1.9} \quad \text{swirl effect}$$

$$\eta_B = 1.22 + 0.08 \ln B_6 \quad \text{aerodynamic blockage effect}$$

where A_6 and A_7 are the passage areas of respectively the inlet and the exit of the diffuser, α_6 is the absolute flow angle at inlet and B_6 is the aerodynamic blockage coefficient at inlet.

3.2 Comparison of Turbine Mean Line Model and CFD

Comparison between mean line model and CFD performance prediction was made for the turbine that was developed for the ORC-ORC prototype. The CFD computations were made using a commercial software, AxCent (Concepts NREC 2010). Results have been compared for several operating conditions and with R134a as working fluid. It appears that the overall performances predicted by the mean line model are very close to the ones calculated with the CFD simulation. Figure 5 shows a comparison of the efficiency and of the power predicted by both methods for an inlet stagnation pressure of 50 bar and an inlet stagnation temperature of 160°C.

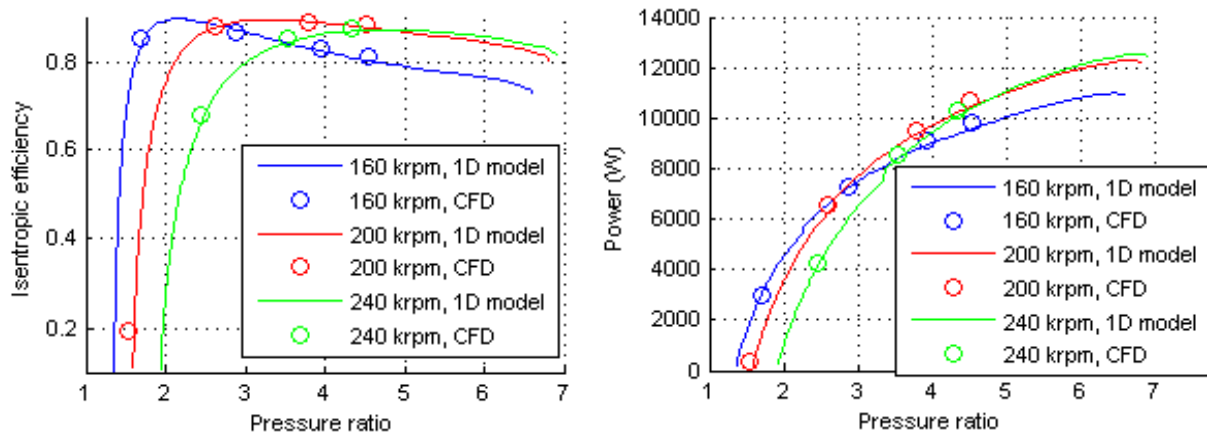


Figure 5: Comparison of the mean line (1D) model and the CFD on the predicted isentropic efficiency and power (inlet stagnation pressure is 50 bar and inlet stagnation temperature is 160°C)

3.3 ORC-ORC Off-design Prediction Example

The inputs to calculate an operating point of the CTU are the inlet stagnation temperature and pressure of the compressor, the mass flow in the compressor, the rotational speed and the inlet stagnation temperature of the turbine. First, the compressor is calculated which sets the power that it requires and the exit stagnation pressure, and thus, the condensing temperature of the cycles. Then, the power losses of the shaft are calculated. With the calculation of those two components, the power that has to be delivered by the turbine is set. Finally, the turbine is calculated in order to reach the required power and exit stagnation pressure. This is done by iterating on the inlet stagnation pressure and either on the mass flow or on the supersonic deviation at nozzle exit or at rotor exit depending on the choke locations. Once, the CTU is calculated, it is possible to determine the thermodynamic state of each point of the cycles.

Figure 6 shows the predicted map of the experimental ORC-ORC prototype but with a turbine nozzle throat area that is the half of the existing ones. It is calculated for a heat pump evaporation temperature of 0°C and a turbine inlet stagnation temperature of 120°C. The map of Figure 6 plots the condensing temperature that can be reached as a function of the COP. The COP calculated here does not integrate the heat sources and the heat sinks like in the previous section. It is simply the ratio of the heat rejected by the condenser and the heat supplied to the evaporator of the ORC plus the power given to the pump. The interesting part of this map is the left side where the temperature increase becomes useful for residential heating applications. The different lines are the iso-velocity curves. They are limited on the left side by compressor surge and on the right side by compressor choke. As it was shown in the previous section (see Figure 3), the rotational speeds required by R1234yf, R236fa and R227ea are lower than required by R134a for the same temperature lift. R1234yf and R236fa

allow to target the same temperature lifts for similar rotational speeds. R227ea has the lowest rotational speeds. The maximum temperature lift is about 35°C, which is just enough for an application with brine source cooled from 4°C to 1°C. The COP values are much lower than the values shown in Figure 3, because here the parameters of the system and the compressor and turbine geometry are not optimized.

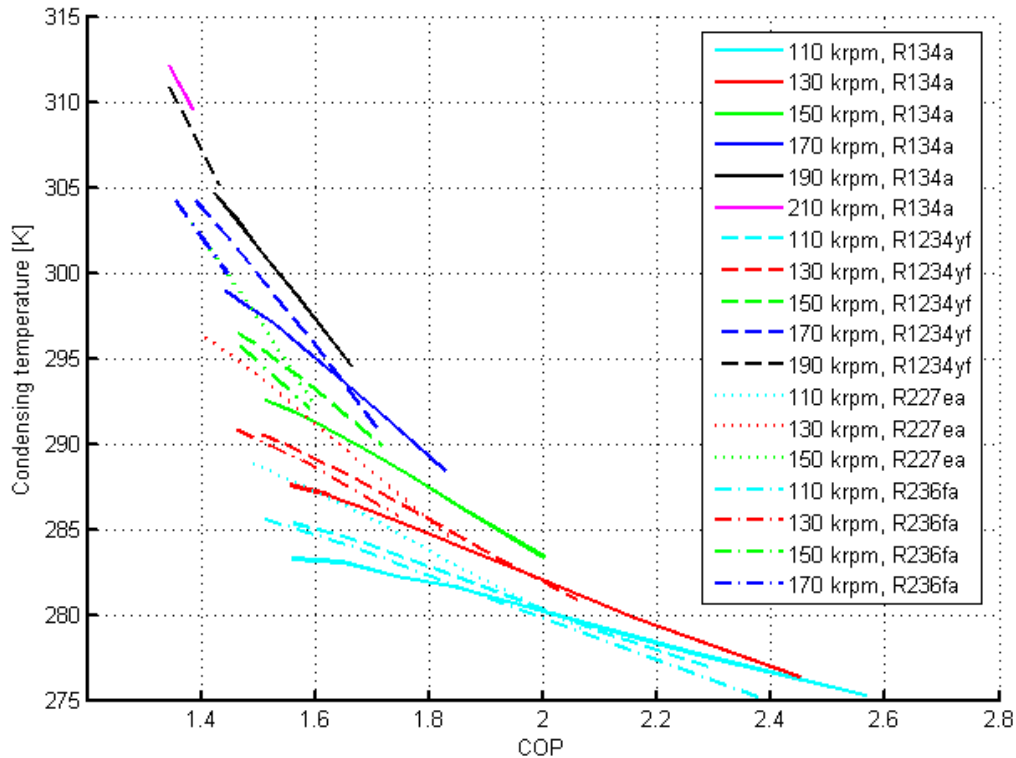


Figure 6: Predicted map of the ORC-ORC experimental prototype for different working fluids (heat pump evaporation temperature is 0°C and turbine inlet stagnation temperature is 120°C)

4 CONCLUSION

An approach to compare the potential of different refrigerants as working fluids for an ORC-ORC thermally driven heat pump has been described. A comparison is presented for an application of residential heating (about 40 kW). This comparison is made on the maximum COP that can be achieved and the minimum rotational speed that is required. Rotational speed is a key parameters for the feasibility of the system, as for small turbomachines the operating speed is critically high. It appears that the best candidates are R134a (COP = 2.33 @ 226 krpm), R1234yf (COP = 2.32 @ 198 krpm), R227ea (COP = 2.36 @ 163 krpm) and R236fa (COP = 2.40 @ 160 krpm).

An off-design radial turbine model is presented. It appears that performance predictions are very close to the ones predicted by CFD analysis. This model, together with previously developed models of the compressor and the shaft loss, enables to simulate off-design operation of ORC-ORC heat pumps. Performance evaluations of the existing experimental prototype have been performed for the four refrigerants mentioned above thanks to this off-design model. From the simulation results, it can be inferred that the existing compressor is capable of reaching the required temperature lift (about 35°C).

First tests of the experimental ORC-ORC prototype were performed at rotational speeds up to 140 krpm. Several technical difficulties were encountered and solved. The next step will be the test of the prototype at rotational speeds up to 200 krpm.

5 ACKNOWLEDGMENTS

The authors would like to thank the *Swiss Federal Office of Energy (OFEN)* for its financial support and *Fischer Engineering Solutions AG* in Herzogenbuchsee (BE, Switzerland) to have supplied the gas bearings and to have assembled and balanced the compressor-turbine unit.

6 REFERENCES

- Baines N.C. 2006. Radial Turbines (course notes), Concepts ETI, Inc., White River Junction, USA.
- Balje O.E. 1981. Turbomachines: A Guide to Design, Selection and Theory, John Wiley & Sons, New York, USA.
- Borel L., D. Favrat 2010. Thermodynamics and energy systems analysis, EPFL Press, Lausanne, Switzerland.
- Concepts NREC. 2010. AGILE Engineering Design System, <http://www.conceptsnrec.com>.
- Demierre J., D. Favrat 2008. "Low power ORC-ORC systems for heat pump applications", *Proc. of the 9th Int. IEA Heat Pump Conf.*, Zürich, Switzerland.
- Lemmon E.W., M.L. Huber, M.O. McLinden 2010. REFPROP - NIST Standard Reference Database 23, Version 9.0, National Institute of Standards and Technology, USA.
- Marechal F., et al. 2004. "Thermo-economic modeling and optimization of fuel cell systems", *Fuel Cells: From Fundamentals to Systems*.
- Molyneaux A., G. Leyland, D. Favrat 2010. "Environomic multi-objective optimisation of a district heating network considering centralized and decentralized heat pumps," *Energy*, 35(2):751–758.
- Moustapha H., M.F. Zelesky, N.C. Baines, D. Japikse 2003. Axial and Radial Turbines, Concepts NREC, White River Junction, USA.
- Rohlik H.E. 1968. "Analytical determination of radial inflow turbine design geometry for maximum efficiency", NASA TN D-4384.
- Schiffmann J. 2008. "Integrated design, optimization and experimental investigation of a direct driven turbocompressor for domestic heat pumps", Ph.D. Thesis, Ecole Polytechnique Fédérale de Lausanne, Switzerland.
- Schiffmann J., D. Favrat 2009. "Experimental investigation of a direct driven radial compressor for domestic heat pumps", *Int. J. of Refrigeration*, 32(8):1918–1928.
- Strong D.T.G. 1980. "Development of a directly fired domestic heat pump", Ph.D. Thesis, University of Oxford, UK.
- Wasserbauer C.A., A.J. Glassman 1975. "FORTRAN program for predicting the off-design performance of radial inflow turbines", NASA TN-8063.
- Whitfield A., N.C. Baines 1990. Design of Radial Turbomachines, Longman Scientific & Technical, Harlow, UK.

Part of

Thermally driven heat pumps for heating and cooling. – Ed.: Annett Kühn – Berlin:
Universitätsverlag der TU Berlin, 2013

ISBN 978-3-7983-2686-6 (print)

ISBN 978-3-7983-2596-8 (online)

urn:nbn:de:kobv:83-opus4-39458

[<http://nbn-resolving.de/urn:nbn:de:kobv:83-opus4-39458>]